ISSN1027-5495. Functional Materials, 30, No.4 (2023), p. 561-570
doi:http://dx.doi.org/10.15407/fm30.04.561

Mechanical properties of ultra-high-performance concrete containing fiber and metakaolin and its predictive modeling study

Changshun Zhou[1], Ziyi Bai[1], Mingyong Li[1], Xudong Wang[1], Chenhui Jiang[2]

[1]Yuanpei College, Shaoxing University, Shaoxing 312000, China
[2] School of Civil Engineering, Shaoxing University, Shaoxing 312000, China

Received August 8,2023

This paper investigates the influence of metakaolin (MK) and different fiber compounds on the mechanical properties of ultra-high performance concrete (UHPC). The study examines the incorporation of MK in combination with steel fibers, glass fibers, polyvinyl alcohol fibers, polypropylene fibers, and continuous basalt fibers, each at a 2% volume fraction in UHPC. The results demonstrate that the addition of MK with steel fibers yields the most favorable mechanical properties, resulting in a remarkable 28% increase in compressive strength, a 14% increase in flexural strength, and a 17.2% increase in modulus of elasticity, compared to specimens without fibers but containing 10% MK. Conversely, the inclusion of other fiber types leads to varying degrees of reduction in the mechanical properties of UHPC. This reduction is attributed to the formation of a weak interface between the fibers and the matrix, as well as fiber agglomeration. The results highlight the importance of careful fiber selection and compatibility of fibers when combining with MK to achieve optimal enhancement in UHPC performance. Based on the experimental test data, a model for predicting the elasticity modulus of UHPC as a function of time and SCMs was proposed with good reliability.

Keywords: ultra-high performance concrete; fiber; mechanical properties; model prediction

Механічні властивості надвисокоякісного бетону, що містить фібру та метакаолін, та їх прогнозне моделювання. *Changshun Zhou, Ziyi Bai, Mingyong Li, Xudong Wang, Chenhui Jiang*

Досліджується вплив метакаоліну (МК) та різних волокнистих сполук на механічні властивості бетону надвисоких експлуатаційних характеристик (UHPC). У дослідженні розглядається включення МК у поєднанні зі сталевими волокнами, скляними волокнами, волокнами полівінілового спирту, поліпропіленовими волокнами та безперервними базальтовими волокнами, кожне з об'ємною часткою 2% UHPC. Результати показують, що додавання МК зі сталевими волокнами дає найбільш сприятливі механічні властивості, що призводить до значного збільшення міцності на стиснення на 28%, міцності на вигин на 14% і збільшення пружності модуля на 17,2% в порівнянні з зразками без волокон, але із вмістом 10% МК. І навпаки, включення інших типів волокон призводить до різного ступеня зниження механічних властивостей UHPC. Це зменшення пов'язане з утворенням слабкої межі між волокнами та матрицею, а також агломерацією волокон. Отримані результати наголошують на важливості ретельного вибору та сумісності волокон при поєднанні з МК для досягнення оптимального підвищення продуктивності UHPC. На основі даних експериментальних випробувань запропоновано модель прогнозування з високою достовірністю модуля пружності UHPC в залежності від часу та СКМ.

1 Introduction

With the ongoing advancement of society, the challenges posed by complex construction projects have exposed the limitations of ordinary concrete's adaptability [1]. To address these issues, experts and scholars have undertaken efforts to enhance and upgrade concrete technology. By incorporating mineral admixtures and chemical additives into ordinary concrete, a new type of concrete with significantly improved strength and superior durability has been developed [2]. Additionally, in order to mitigate the effects of material heterogeneity on concrete performance, some researchers have taken a step further, eliminating the use of coarse aggregate and instead substituting it with well-graded quartz sand to produce what is known as ultra-high performance concrete (UHPC) [3, 4]. This innovative approach has produced a concrete with exceptional properties, exhibiting outstanding mechanical properties and durability. [5]. The development of UHPC represents a promising solution to meet the requirements of modern construction projects, providing a highly adaptive and durable material for various challenging applications in the construction industry [6].

The researches indicate that UHPC exhibits significant variations in compressive strength (200~800MPa), tensile strength (25~150MPa), and bending strength (30~140MPa). These properties are influenced by various factors, including the choice of raw materials, pouring quality, and curing conditions [7, 8]. Yazıcı et al. [9] demonstrated that the inclusion of steel fibers enhances the flexural load-bearing capacity of UHPC, particularly after reaching the peak load. Similarly, the addition of blast furnace slag in UHPC improves its flexural strength due to the significantly improved bond strength between the UHPC matrix and fibers. Yoo et al. [10] found that steel fibers play a crucial role in preventing the formation of micro-cracks and limiting the propagation of macro-cracks, thus leading to an increase in compressive strength. The optimal dosage of steel fibers is determined to be 3%. Moreover, Sim and Park [11] reveals that the incorporation of basalt fibers in UHPC results in approximately 27% higher yield strength and ultimate strength in flexural strength tests. On the contrary, Rigaud et al. [12] discovered that excessive amounts of glass fibers or agglomeration during the mixing process can have adverse effects on the strength of UHPC. The application potential of UHPC is vast, but its widespread adoption is constrained by various factors. Notably, UHPC with low water-binder ratio requires a substantial dosage of cementitious material (1100-1300 kg/m^3) and silicon powder (200-350 kg/m^3). However, the degree of cement hydration remains relatively low at only 30-35%. The significant amount of jelly-like material in UHPS simply serves as a filler for the microaggregates. Consequently, the cost of UHPC is significantly higher than that of ordinary concrete, and its extensive use of cement contributes to increased CO_2 emissions. In conclusion, while UHPC possesses remarkable properties for various applications, its adoption on a large scale is still limited due to factors such as cost, cement usage, and environmental concerns. Further research and development efforts are essential to improve its cost-effectiveness and reduce its environmental impact, ultimately facilitating its broader utilization in the construction industry.

Metakaolin (MK) is a pozzolanic material derived from the calcination of kaolin at temperatures ranging from 500°C to 800°C. Kaolin serves as the primary raw material for producing metakaolin ($Al_2Si_2O_7$). The process involves calcining kaolin at 600°C for 6 hours or at 700-900°C for more than 2 hours, resulting in the formation of metakaolin [13, 14]. Metakaolin exists as a transitional phase with lower crystallinity while retaining the lamellar structure of kaolin. However, the flaky and tubular crystals become smaller, imparting excellent gelling activity to metakaolin. Extensive research has consistently shown that incorporating MK in concrete as a supplementary cementitious material can enhance the mechanical properties of the concrete. The positive effect is observed when MK replaces a portion of the cement in the mixture. However, the optimal dosage of MK for achieving this positive effect is typically within the range of 10% to 20%. If the MK dosage exceeds this range, the mechanical properties of the concrete are likely to experience a notable reduction [15]. Courard et al. [16] obtained similar results in their study on cement mortar. The sample containing 20% MK showed a slight decrease in bending strength during the early stage (3 days) of curing. However, after 14 days of curing, the bending strength of the mortar with 20% MK exceeded the strength of the control sample. In conclusion, MK demonstrates significant potential as an auxiliary cementitious material to enhance the mechanical properties of concrete. Its optimal dosage should be carefully considered to achieve the desired positive effects on concrete performance. Beyond the recommended range, an excessive amount of MK

Table 1 Physical properties and chemical composition of cementitious materials

Sample	Physical properties		Chemical components								
	Specific surface area, m^2/kg	Densityg/cm	SiO_2	Al_2O_3	Fe_2O_3	CaO	MgO	SO_3	K_2O	Na_2O	L.O.I
Cement	381	3.25	23.25	5.46	3.71	59.52	3.5	2.2	0.21	0.52	0.82
MK	20000	2.6	54	43	0.8	0.22	0.61	0.14	0.16	0.14	0.5
SF	22315	3.1	93.86	1.2	0.64	0.2	0.25	0.64	0.23	0.45	2.26

Table 2 Characteristics of various fiber materials

Fiber material	Material properties					
	Length /mm	Diameter /μm	Density /kg/m^3	Tensile strength /MPa	Elastic Modulus /GPa	Elongation at break /%
SL	13	220	7.8	2800	210	3.6
GF	12	30	2.5	350	4.3	24
PVA	12	35	0.9	630	6	18
PP	12	15.09	1.29	1830	40	6.9
CB	12	17	2.5	2300	86	2.6

may lead to a decline in mechanical properties. Understanding and controlling the appropriate dosage of MK is vital to harness its beneficial effects in concrete mixtures.

This paper presents the results of an experimental study of mechanical properties of UHPC. The research considers incorporating five different fiber materials, namely steel fibers (SL), glass fibers (GF), polyvinyl alcohol fibers (PVA), polypropylene fibers (PP), and continuous basalt fibers (CB), along with MK, into the UHPC matrix. Various samples were prepared, and their compressive strength, flexural strength, and elastic modulus were measured after 7 days, 28 days, and 90 days of curing. The experimental data obtained from the tests were then compared with the existing elastic modulus prediction model. Based on the comparison and analysis of the experimental results, a novel model for predicting the elastic modulus of UHPC over time was proposed. This study contributes to the existing knowledge and understanding of UHPC and opens possibilities for further advancements in the design and application of this UHPC in various engineering and construction applications. The research outcomes can potentially lead to the development of more reliable and durable concrete structures by optimizing the mix design and considering the time-dependent behavior of UHPC.

2 Experimental

2.1 Raw materials

In this test, several materials were used, including cement with a designation of P O 52.5, MK from Shanghai Haofu Chemical Co., Ltd., and micro silica fume (SF) from Sichuan silica fume production plant. Table 1 presents the physical and chemical properties of these materials, and Figure 1 displays the SEM images of cement, MK, and SF. Various fiber materials were employed in this study, namely SL, GF, PVA, PP, and CB. Table 2 provides the characteristics of each fiber material, and Figure 2 shows the physical appearance of these fibers. For the fine aggregate, ISO standard sand was used. The water reducer utilized in the test is a polycarboxylate water reducer (PC) with a solid content of approximately 28% and a water reducing rate of 25%. As for the mixing water, it was sourced from tap water.

2.2 Mix Ratio Design

The objective of this study was to investigate the impact of MK and five different fiber materials, namely SL, GF, PVA, PP, and CB, on the mechanical properties of UHPC. Each fiber material was added to the UHPC mix at a volume fraction of 2%. The water-to-binder ratio (w/b) used in the UHPC samples was 0.15, and the cement-to-cement ratio was 0.65. To maintain consistency in fluidity, the amount of super-

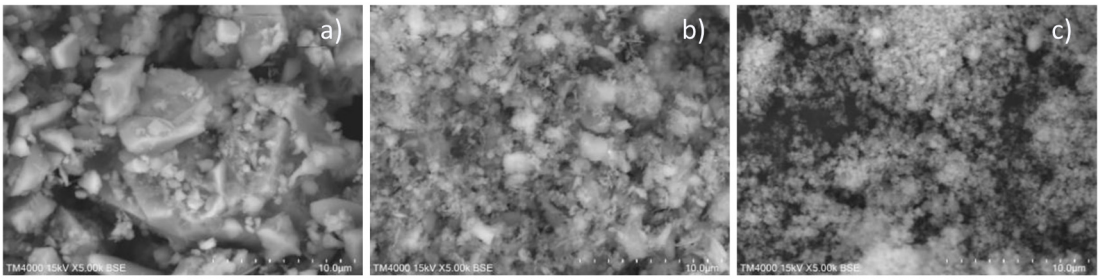

Fig.1 SEM image (a) cement; (b) MK; (c) SF

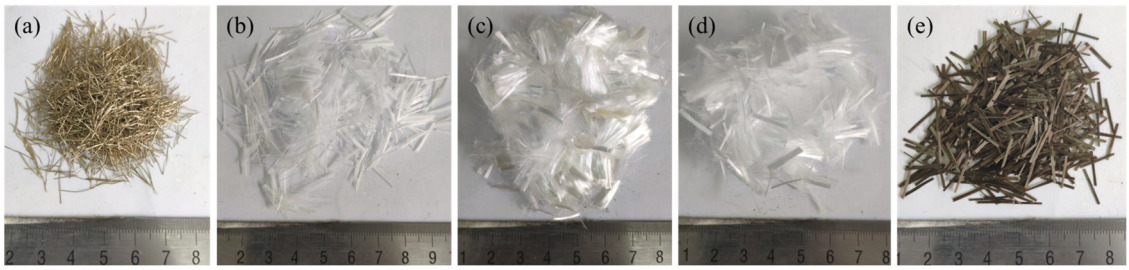

Fig 2 Physical map of fiber materials (a) SL, (b) GF, (c) PVA, (d) PP and (e) CB

Table 3 UHPC mix ratio design

No.	Material, kg/m^3						Fiber content, volume fraction, V/%				
	Cement	SF	MK	Sand	Water	PC	SL	GF	PP	PVA	CB
MK0	1080	120	0	780	180	40	/	/	/	/	/
MK10	960	120	120	780	180	40	/	/	/	/	/
MK10-SL	960	120	120	780	180	40	2%	/	/	/	/
MK10-GF	960	120	120	780	180	40	/	2%	/	/	/
MK10-PP	960	120	120	780	180	40	/	/	2%	/	/
MK10-PVA	960	120	120	780	180	40	/	/	/	2%	/
MK10-CB	960	120	120	780	180	40	/	/	/	/	2%

plasticizer in the samples was adjusted based on the fluidity of the benchmark group, ensuring that the slump flow of the UHPC remained within the range of 220-240 mm. The specific mixing ratios of UHPC used in the study are presented in Table 3.

2.3 Test Method

The test method employed in this study follows the standard rubber sand test procedure. For each UHPC sample, cubic specimens measuring 40×40×160 mm are prepared. These specimens are then subjected to curing in a standard curing room until they reach the desired test age, which includes 7 days, 28 days, and 90 days. At each specified test age, the compressive strength, flexural strength, and elastic modulus of the UHPC samples are measured.

3. Results and discussion

3.1 Compressive strength

Fig. 3a presents the impact of metakaolin (MK) and different fiber combinations on the compressive strength of UHPC. It can be seen from the figure that the compressive strength of the sample containing 10% MK after 7 days is nearly equivalent to that of the sample without MK. However, after 28 days, the compressive strength with MK10 increases by 20.1%. This improvement can be attributed to the phenomenon of "secondary hydration" occurring between SiO_2, Al_2O_3, and CH crystals in the MK. This reaction generates additional calcium silicate hydrate (C-S-H) and calcium aluminate hydrate, filling the pores in the matrix and resulting in a more compact microstructure of the UHPC matrix [17]. Furthermore, there are dis-

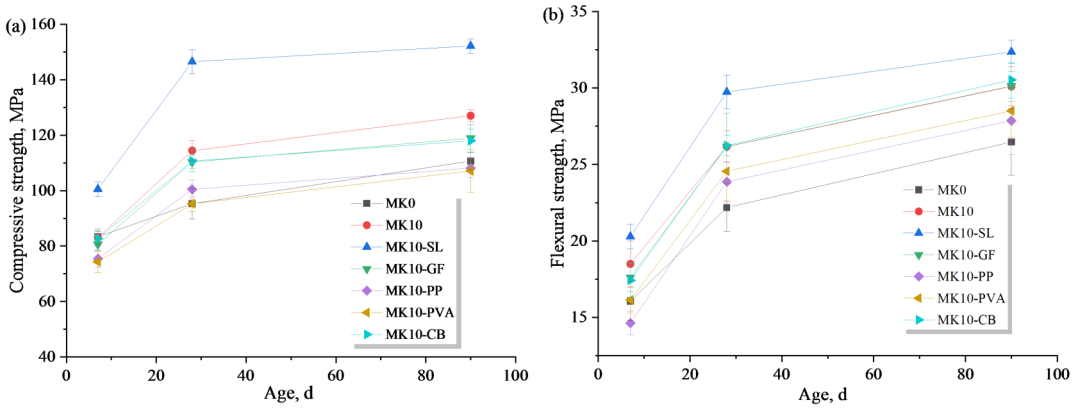

Fig.3 Effect of MK and fiber on (a) the compressive strength and (b) the flexural strength of UHPC

tinct differences in the effects of MK and the various fiber combinations on the compressive strength of UHPC. The inclusion of steel fibers consistently leads to the highest strength in UHPC. In comparison to MK10, the compressive strength of sample MK10-SL after 7 days, 28 days and 90 days increases respectively by 21%, 28% and 18.2%.

Fig. 3b displays the effect of MK and various fiber combinations on the flexural strength of UHPC. The results reveal that the flexural strength of MK10 samples after 7 days, 28 days, and 90 days increased by 10%, 18%, and 13.7%, respectively, compared to MK0 samples. However, the incorporation of different fiber materials leads to distinct changes in UHPC's flexural strength. For the MK10-SL samples, the flexural strength at 7 days, 28 days, and 90 days increased by 10%, 14%, and 8%, respectively, compared to the MK10 sample. The inclusion of MK10-GF and MK10-CB significantly impacted the flexural strength of UHPC, particularly in the later stages, exhibiting a strengthening effect with flexural strengths at 28 days and 90 days slightly higher than those of the MK10 and MK0 samples. This effect can be attributed to the bridging and anchoring functions of GF and CB within the matrix, which hinder the further development of microcracks. In contrast, the flexural strengths of MK10-PP and MK10-PVA samples after 28 days and 90 days decreased by 9%, 6%, and 7.4%, 5%, respectively, compared to the MK10 samples. However, these values remain slightly higher than those of the MK0 samples. This decrease in flexural strength may be due to the smooth surface of PP and PVA, which result in the formation of weak interfaces and uneven agglomeration in the interfacial transition zone with the matrix.

The observed phenomena in the flexural strength of UHPC with different fiber combinations and MK content can be attributed to various factors:

(1) Reinforcing Effect of SL: SL play a significant role in enhancing the flexural strength of UHPC. The bridging effect of steel fibers at cracks slows down the crack growth rate, increasing the bearing capacity of UHPC as the crack width increases. This reinforcement mechanism is beneficial for UHPC's flexural strength improvement.

(2) Effect of GF: GF has a lower elastic modulus compared to steel fiber, resulting in a relatively weaker impact on the strength of UHPC. While a small amount of glass fiber can improve the strength of the concrete matrix to some extent, excessive content, or the occurrence of fiber agglomeration during the mixing process can adversely affect the concrete strength. Studies have shown that when the glass fiber content is below 2%, there is a maximum increase in concrete strength of about 11.3%. However, as the glass fiber content exceeds 2%, the concrete strength gradually decreases, with a maximum reduction rate of around 16.6% [18, 19].

(3) Weak Bond Strength of CB: The bond strength between basalt fiber and the UHPC matrix is weaker compared to other fiber materials. When the amount of basalt fiber is too high, the matrix may not be filled around the fibers, which leads to a decrease in the compactness of the UHPC matrix and, subsequently, a decrease in strength [20].

(4) Effect of PPA: Excessive amounts of PP and PVA can cause their own dispersion to overwhelm the contribution of the fiber itself to the compressive strength. This leads to an increased number of weak interfaces within the material. When subjected to pressure, these weak inter-

faces preferentially crack, resulting in a decrease in the compressive strength of UHPC.

The combination of different fiber materials with MK in UHPC introduces various reinforcing and weakening effects, leading to the observed differences in the flexural strength at different curing ages. Understanding these factors helps in optimizing fiber content and selection to achieve the desired mechanical properties in UHPC mix designs.

3.2 Elastic Modulus

Fig. 4 illustrates the effect of MK and different fiber combinations on the elastic modulus of UHPC. It can be seen that the elastic modulus of MK10 samples after 7 days, 28 days, and 90 days increases by 3%, 12.8%, and 9.4%, respectively, compared to MK0 samples. After the incorporation of steel fibers, the elastic modulus of UHPC shows significant improvement. The elastic modulus of MK10-SL samples after 7 days, 28 days, and 90 days increases by 16.7%, 17.2%, and 13.3%, respectively, compared to MK10 samples. For MK10-GF and MK10-CB samples, their change trends are very similar, and their elastic modulus is slightly higher than that of MK10 in the early stage. However, with age, their elastic modulus decreases. These results indicate that the effect of glass fibers and basalt fibers on the elastic modulus of UHPC is positive in the early stages but diminishes over time. This could be attributed to the bonding and anchoring functions of these fibers, which initially hinder crack development, but their limited contribution to long-term strength causes a decrease in elastic modulus. Furthermore, the elastic modulus of MK10-PP and MK10-PVA samples shows similar trends. After 7 days, 28 days, and 90 days, the elastic modulus of these samples decreases by 11.6%, 7%, and 6.3%, and 5.3%, 10.5%, and 8.8%, respectively, compared to the MK10 samples. This can be attributed to the lower elastic modulus of organic fibers (PP and PVA) and their limited contribution to the overall strength of UHPC. Additionally, the occurrence of agglomeration of these fibers can increase the pore structure within the matrix, leading to a reduction in the mechanical properties of UHPC.

3.3. Analysis of Elastic Modulus Prediction Model

The static elastic modulus of concrete is a critical parameter that reflects the instantaneous stress-strain relationship and is closely

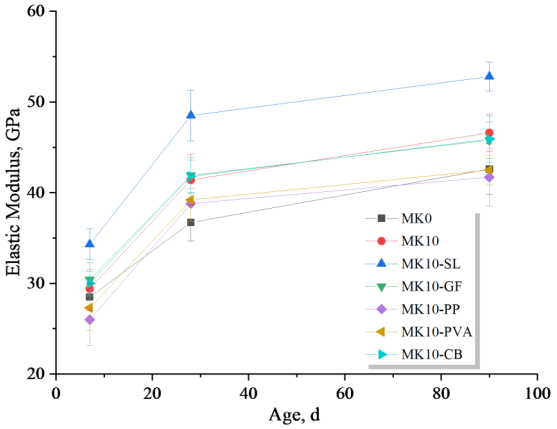

Fig 4. Effect of MK and fiber on the Elastic modulus of UHPC

related to the compressive strength of the material. Accurate prediction of the static elastic modulus is essential for designers to calculate prestress losses, deflection, and displacement in concrete structures. Currently, there are two main types of prediction models for the elastic modulus of concrete:

Compressive Strength-Based Models (Models-1): These models predict the elastic modulus of concrete, based on its compressive strength at different ages. The compressive strength is often considered the main indicator of the mechanical properties of concrete, and its relationship with the elastic modulus has been studied extensively.

Time-Based Models (Models-2): These models represent the elastic modulus as a function of time. Time-dependent behavior is considered, recognizing that the elastic modulus of concrete evolves over time due to ongoing hydration and structural changes.

In this section, the existing test results for compressive strength and elastic modulus are compared with two existing elastic modulus prediction models. The goal is to propose a new model suitable for UHPC, containing various additives, based on traditional models. The proposed model takes into consideration the specific characteristics of UHPC, including the influence of MK and different fiber materials on its mechanical properties. By incorporating these factors into the model, a more accurate and tailored prediction of the elastic modulus of UHPC at various ages will be offered. This new elastic modulus prediction model will provide valuable insights for designing UHPC-based structures, allowing engineers to make more informed decisions regarding prestress loss, deflection, and displacement, thereby ensuring

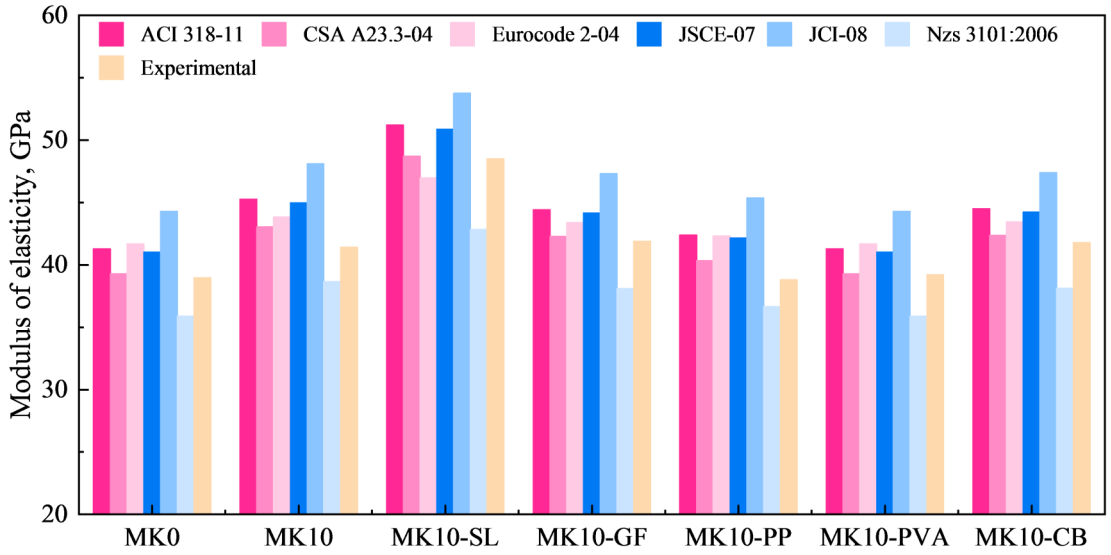

Fig.5. Comparison of Models-1 and experimental UHPC elastic modulus after 28d

the overall performance and safety of concrete structures containing MK and various fiber materials.

To evaluate the effectiveness of the concrete elastic modulus prediction model Models-1 (Table 4), the elastic modulus of UHPC after 28 days was taken as an example, and its test value (E_c) was compared with the predicted value (E_c') of the model, as shown in Fig. 5. Upon examination of the comparison chart, it is evident that the results from the elastic modulus prediction model still significantly differ from the actual test value. The JCI-08 model consistently overpredicts the elastic modulus (E_c'), with a deviation range from the test value (E_c) within 11% to 17%. The predictions from ACI 318-11, Eurocode 2-04, JSCE-07, and JCI-08 models are slightly higher than the experimental value (E_c), with a deviation range below 10%. On the other hand, the Nzs 3101:2006 model tends to underpredict values, while the predictions of the CSA A23.3-04 model are very close to the actual test value. These results highlight that the existing elastic modulus prediction models (Models-1) may not fully capture the complex behavior of UHPC containing different admixtures, such as metakaolin and various fiber materials. As a result, the predicted elastic modulus values (E_c') tend to deviate from the actual test values (E_c). To improve the accuracy of the prediction model for UHPC, it is necessary to develop a new model that accounts for the specific effects of metakaolin and various fiber materials on the mechanical properties of UHPC. This customized model could yield more precise predictions of the elastic modulus at different ages, thereby enhancing the applicability and reliability of the model for UHPC mix designs and structural evaluations.

Table 4. Summary of conventional concrete mechanical property models (Models-1).

Model	Elastic modulus (E_c') (GPa)
ACI 318-11 [21]	$E_c'=4.73f_c'^{1/2}$
CSA A23.3-04 [22]	$E_c'=4.5f_c'^{1/2}$
Eurocode 2-04 [23]	$E_c'=22((f_c'+8)/10)^{0.3}$
JSCE-07 [24]	$E_c'=4.7f_c'^{1/2}$
JCI-08 [25]	$E_c'=6.3f_c'^{0.45}$
Nzs 3101:2006 [26]	$E_c'=3.32(f_c'^{1/2})+6.9$
f_c'= Compressive strength of 28d cylindrical concrete, MPa; f_c = Compressive strength of cube concrete 28d, MPa; $f_c=1.25f_c'$ [27, 28].	

Based on the analysis above, it is evident that the prediction of elastic modulus using Models-1, which relies on the known compressive strength at different ages, can increase the amount of prediction and calculation work for concrete. To address this, some scholars have studied concrete elastic modulus prediction models (Models-2) over time, as shown in Table 5. Fig. 6 presents a comparison between the test values of UHPC elastic modulus and the prediction models for ordinary concrete. The comparison reveals a substantial difference between the predicted values of the elastic modulus for ordinary concrete and the UHPC test values. Table 5 shows the deviation val-

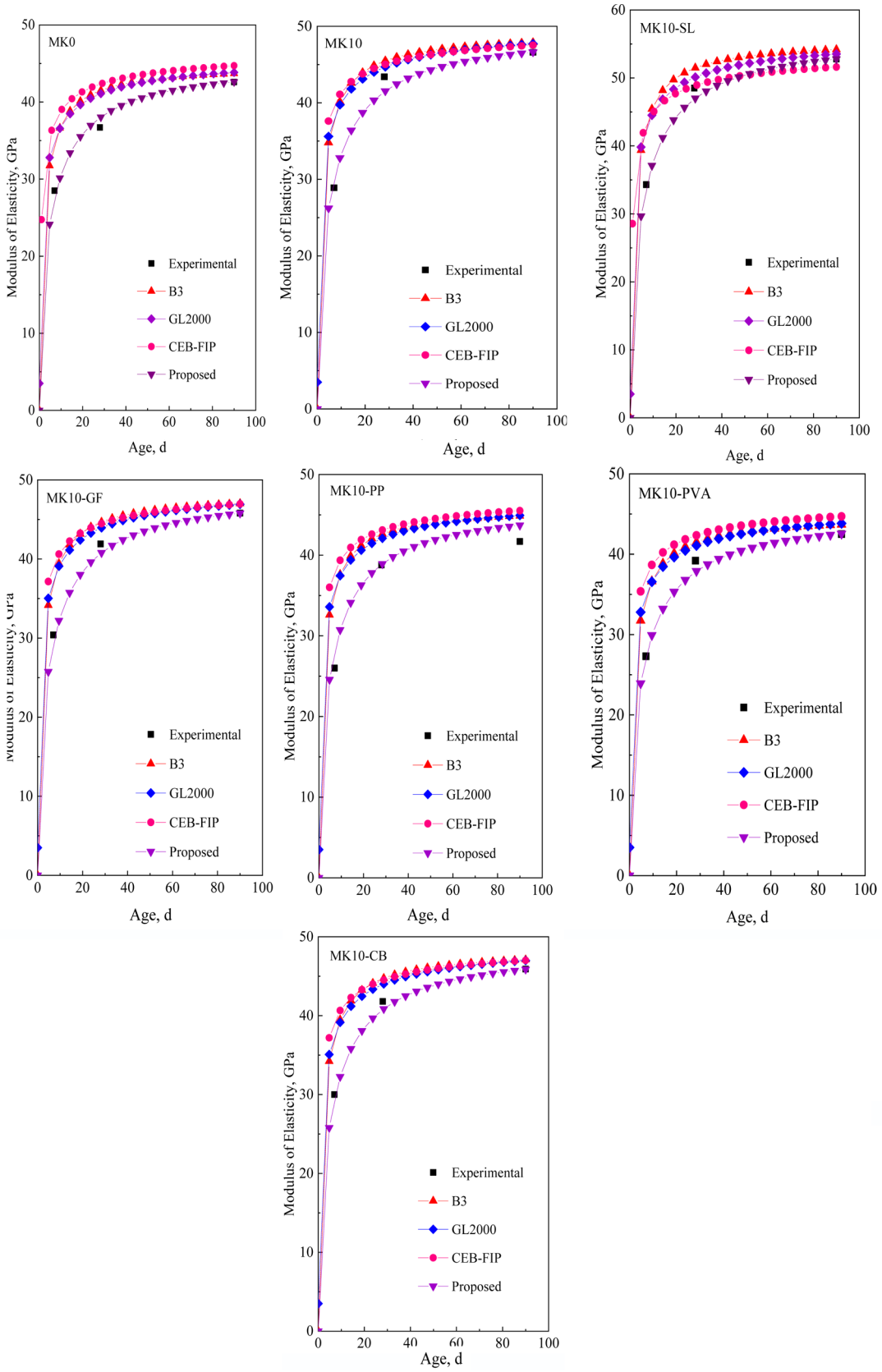

Fig.6 Evolution of elastic modulus of UHPC with age for mix group.

Table 5. Models for time dependent modulus of elasticity of concrete.

Source	Modela (GPa)	Deviation from test value		
		7d	28d	90d
B3[30-32]	$E_c'=4.734(f_c' \cdot T/(4+0.85T))^{0.5}$	21%~37%	6%~13%	2.6%~7.6%
GL2000[33]	$E_c'=3.5+4.3(f_c' \cdot T^{0.75}/(2.8+0.77T^{0.75}))^{0.5}$	22%~29%	3.2%~11.8%	1.4%~5.7%
CEB-FIP[34]	$E_c'=21.5(f_c'/10)^{1/3} \cdot (\mathrm{Exp}(0.25\text{-}7/4 \cdot T^{0.5})^{0.5}$	25.6%~46%	6%~15.3%	1.7%~9%
Note: f_{ct}' is the compressive strength of cylindrical concrete at different ages, MPa; T is the age of concrete curing, d; σ is the mass fraction of SCMs.				

ues. The predicted values of the B3 model, GL2000 model, and CEB-FIP model generally exceed the experimental values, with the CEB-FIP model consistently producing higher values than the B3 and GL2000 models, which is consistent with the literature [29]. None of these models can accurately predict the elastic modulus with curing age. Based on these observations, this paper proposes a UHPC elastic modulus prediction model that considers age variation, compressive strength, and mineral admixture content. This model aims to achieve better accuracy in predicting the elastic modulus of UHPC over time. Through multiple regression analysis of the test data, the following best-fit expression was obtained:

$$E_c'=4.5(f_c \cdot T/(22.5(1\text{-}0.5\mathrm{Exp}(\text{-}0.25\sigma))+0.75\ T))^{0.5} \quad (1)$$

Here, f_c is the cubic compressive strength of concrete, MPa; T is the concrete curing age, d; σ is the mass fraction of SCMs. The performance of the new model was evaluated based on estimates of various errors, including the mean error, mean absolute error, maximum absolute error, and maximum deviation; the obtained estimates were found to be 0.4%, 2.1%, 7%, and 1.9 GPa, respectively. Fig.7 displays a comparison between the experimental values and the predicted values using the new UHPC elastic modulus prediction model. It is evident from the figure that most of the data points fall within the error range of ±10%. These results indicate that the proposed model exhibits good accuracy and reliability in predicting the elastic modulus of UHPC over time. Most of the predicted values are in close agreement with the experimental values, validating the effectiveness of the model in identifying the complex behavior of UHPC containing various admixtures.

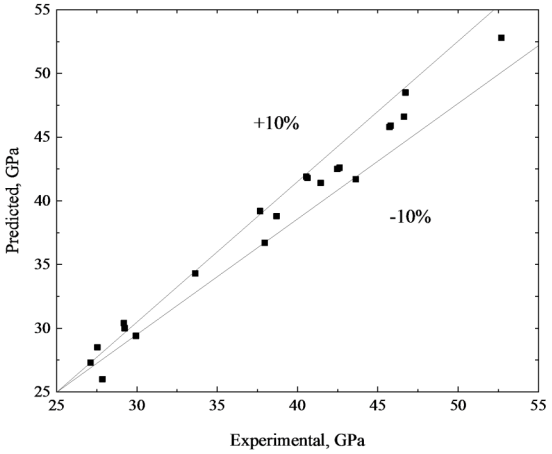

Fig.7 Comparison of experimental and predicted values of static modulus of elasticity with new proposed model

4 Conclusions

(1) The study investigated the influence of MK and different fiber materials on the mechanical properties of UHPC. Steel fibers showed a significant strengthening effect on UHPC, leading to a substantial increase in its 28-day compressive strength, flexural strength, and elastic modulus by 28%, 14%, and 17.2%, respectively. This enhancement was attributed to the high stiffness and strength of steel fibers, as well as their ability to bridge and interlock at cracks, slowing down crack propagation. On the other hand, the incorporation of other fibers resulted in a reduction in the mechanical properties of UHPC. This was mainly due to the weak interface between these fibers and the matrix, as well as the occurrence of fiber agglomeration.

(2) The elastic modulus prediction model was developed using the following best-fit expression $E_c' = 4.5(f_c\ T / (22.5(1 - 0.5\exp(-0.25\sigma)) + 0.75\ T))^{0.5}$ based on the multiple regression analysis of the test data. The study evaluated the performance of the new UHPC elastic modulus prediction model by comparing it with the experimental test values. The various errors of the model, including the mean error, mean absolute error, maximum absolute error, and maximum deviation values, were estimated to

be 0.4%, 2.1%, 7%, and 1.9 GPa, respectively. The results demonstrated that the proposed model achieved good accuracy and reliability in predicting the elastic modulus of UHPC over time. About 90% of the data points were within the error range of ±10%, indicating that the model provided a precise estimation of the elastic modulus for most cases.

Overall, the study provided valuable insights into the mechanical properties of UHPC with various admixtures, highlighting the significant contribution of steel fibers to its strength. The developed new elastic modulus prediction model offers an improved and reliable approach for estimating the elastic modulus of UHPC over time, aiding in the design and evaluation of UHPC-based concrete structures.

Acknowledgements

This work was financially supported by the National Natural Science Foundation of Zhejiang province (Grant No. LHY22E080001).

References

1. P. Zhan, J. Xu, J. Wang, J. Zuo, Z. He, *J. Cleaner Production* **375,** 134116, (2022).
2. P. Zhan, J. Xu, J. Wang, C. Jiang, ete, *Construction and Building Materials* **307,** 125082 **(**2021).
3. M.H. Akeed, S. Qaidi, H.U. Ahmed, R.H. Faraj, A.S. Mohammed, W. Emad, B.A. Tayeh, A.R.G. Azevedo, Ultra-high-performance fiber-reinforced concrete. Part I: Developments, principles, raw materials, Case Studies in Construction Materials 17, e01290 (2022).
4. M.H. Akeed, S. Qaidi, H.U. Ahmed, R.H. Faraj, A.S. Mohammed, W. Emad, B.A. Tayeh, A.R.G. Azevedo, Ultra-high-performance fiber-reinforced concrete. Part II: Hydration and microstructure, Case Studies in Construction Materials **17**,e01289 (2022),.
5. P. Zhan, Z. He, *Construction and Building Materials* **201**, 676, (2019)
6. J. Xu, P. Zhan, W. Zhou, J. Zuo, S.P. Shah, Z. He, *Powder Technol*. **419** , 18356 (2023).
7. O. Bonneau, M. Lachemi, E. Dallaire, J. Dugat, P.-C. Aitcin, *Materials Journal* **94**(4)) 286 (1997).
8. M. Ipek, K. Yilmaz, M. Sümer, M. Saribiyik, *Construction and Building Materials* **25**(1), 61, (2011).
9. H. Yazıcı, M.Y. Yardımcı, H. Yiğiter, S. Aydın, S. Türkel, *Cem. Concr. Compos.* **32**(8) 639 (2010).
10. D.-Y. Yoo, J.-H. Lee, Y.-S. Yoon, Effect of fiber content on mechanical and fracture properties of ultra high performance fiber reinforced cementitious composites, CmpSt 106 (2013) 742-753.
11. J. Sim, C. Park, D.Y. Moon, Characteristics of basalt fiber as a strengthening material for concrete structures, Composites Part B: Engineering 36(6) (2005) 504-512.
12. C.G. Rigaud S, Chen J., Characterization of bending and tensile behavior of ultra-high performance concrete containing glass fibers, High Performance Fiber Reinforced Cement Composites 6, Springer, Dordrecht, 2012.
13. J. Kinuthia, S. Wild, B. Sabir, J. Bai, *Advances in cement research* **12**(1) , 35(2000) 15. E. Guneyisi, M. Gesoglu, A.O.M. Akoi, K. Mermerdas,*Composites Part B-Engineering* **56**-9 (2014) 83 (2003)
16. L. Courard, A. Darimont, M. Schouterden, F. Ferauche, X. Willem, R. Degeimbre, , *Cem. Concr. Res.* **33**(9), 1473 (2003)
17. J.J. Brooks, M.A.M. Johari, Effect of metakaolin on creep and shrinkage of concrete, *Cem. Concr. Compos.* **23(**6), 495 (2001)
18. A.B. Kizilkanat, N. Kabay, V. Akyüncü, S. Chowdhury, A.H. Akça, *Construction and Building Materials* **100**, 218 (2015).
19. P. Zhan, J. Xu, J. Wang, J. Zuo, Z. He,, *Cem. Concr. Compos*. 137, 104924 (2023).
20. S. Kakooei, H.M. Akil, M. Jamshidi, J. Rouhi,, *Construction and Building Materials* **27**(1), 73 (2012)
21. ACI 318-11 Building code requirements for structural concrete and commentary, ACI International, Farmington Hills (Mich), 2011.
22. C. A23.3-04., Building code requirements for structural concrete and commentary, PCA notes on ACI 318-11: with design applications., Farmington Hills (Mich): ACI International, 2011.
23. E. 2-04, Design of concrete structures: Part 1-1: general rules and rules for buildings., British Standards Institution, 2004.
24. JSCE-07, Standard specification for concrete structure., JSCE No. 15, Tokyo, Japan;, 2007.
25. JCI-08, Guidelines for control of cracking of mass concrete 2008, Japan Concrete Institute, 2008.
26. N. 3101:2006, Concrete structures standard. The design of concrete structures., Wellington, New Zealand, 2006.
27. M. Shariq, J. Prasad, H. Abbas , *Construction and Building Materials* **41**, 411 (2013)
28. M. Shariq, J. Prasad, A. Masood, *Construction and Building Materials* **24**(8) , 1469(2010)
31. Z.P. Bazant, S. Baweja, *Mater. Struct.* **28**(8), 488, (1995)
32. Z.P. Bažant, S. Baweja, *Mater. Struct.*, **29(**10), 587 (1996).
33. N.J. Gardner, M.J. Lockman,, *ACI Mater. J.* 98(2), 159, (2001).
34. C.-F.m. code, design code 1994, Thomas Telford, London, 1990.